

# ATXR5 and ATXR6 are H3K27 monomethyltransferases required for chromatin structure and gene silencing

Yannick Jacob<sup>1</sup>, Suhua Feng<sup>2,3</sup>, Chantal A LeBlanc<sup>1</sup>, Yana V Bernatavichute<sup>3,4</sup>, Hume Stroud<sup>3</sup>, Shawn Cokus<sup>3</sup>, Lianna M Johnson<sup>5</sup>, Matteo Pellegrini<sup>3</sup>, Steven E Jacobsen<sup>2-4</sup> & Scott D Michaels<sup>1</sup>

Constitutive heterochromatin in *Arabidopsis thaliana* is marked by repressive chromatin modifications, including DNA methylation, histone H3 dimethylation at Lys9 (H3K9me2) and monomethylation at Lys27 (H3K27me1). The enzymes catalyzing DNA methylation and H3K9me2 have been identified; alterations in these proteins lead to reactivation of silenced heterochromatic elements. The enzymes responsible for heterochromatic H3K27me1, in contrast, remain unknown. Here we show that the divergent SET-domain proteins ARABIDOPSIS TRITHORAX-RELATED PROTEIN 5 (ATXR5) and ATXR6 have H3K27 monomethyltransferase activity, and *atxr5 atxr6* double mutants have reduced H3K27me1 *in vivo* and show partial heterochromatin decondensation. Mutations in *atxr5* and *atxr6* also lead to transcriptional activation of repressed heterochromatic elements. Notably, H3K9me2 and DNA methylation are unaffected in double mutants. These results indicate that ATXR5 and ATXR6 form a new class of H3K27 methyltransferases and that H3K27me1 represents a previously uncharacterized pathway required for transcriptional repression in *Arabidopsis*.

In eukaryotes, chromatin modifications such as the methylation of DNA and specific histone residues are associated with epigenetic gene silencing and heterochromatin formation<sup>1</sup>. Nuclei of the model plant *Arabidopsis thaliana* contain highly condensed regions of constitutive heterochromatin referred to as chromocenters, which are primarily composed of pericentromeric repeats, transposons and ribosomal DNA genes<sup>2</sup>. Chromocenters are enriched with several epigenetic marks, including DNA methylation at CG, CHG and CHH (where H represents A, T or C) sites, as well as histone modifications such as dimethylation at histone H3 Lys9 (H3K9me2) and monomethylation at histone H3 Lys27 (H3K27me1)<sup>3-7</sup>. The enzymes responsible for the establishment and the maintenance of DNA methylation include DOMAINS REARRANGED METHYLASE 2, which is responsible for the establishment of DNA methylation in all three sequence contexts<sup>8,9</sup>, and METHYLTRANSFERASE 1 (MET1) and CHROMO-METHYLASE 3, which are required for proper maintenance of CG and CHG methylation, respectively<sup>10-12</sup>. Dimethylation at H3K9 is mediated by SU(VAR) homologs (SUVH), such as SUVH2, KRYPTONITE (KYP; also known as SUVH4), SUVH5 and SUVH6 (refs. 11,13-15). The lower level of H3K9me2 in a *kyp* mutant leads to lower levels of DNA methylation at some loci, suggesting a link between DNA and histone methylation<sup>11,16</sup>. Removal of DNA methylation or H3K9me2 leads to transcriptional activation of transposable and repeat elements<sup>17</sup>. In contrast to H3K9me2, the role of H3K27me1 at chromocenters is less well understood. Data suggest, however, that H3K27me1 is likely to be present independent

of DNA methylation or H3K9me2, as H3K27 methylation is unaffected in *kyp* and *met1* mutants<sup>18,19</sup>.

The role of H3K27me1 presents a major unanswered question with respect to the chromatin modifications associated with *Arabidopsis* chromocenters. Studies addressing the significance of this mark have been hampered by the inability to identify the enzymes responsible for H3K27me1. The eukaryotic enzymes that methylate H3K27 *in vivo* are all homologs of the *Drosophila melanogaster* SET-domain protein Enhancer of zeste (E(Z))<sup>20</sup>. E(Z) acts as part of the Polycomb repressive complex 2 (PRC2) and requires the WD-40 protein Extra sex combs for activity in *Drosophila*<sup>21</sup>. *Arabidopsis* contains three E(Z) homologs: MEDEA (MEA), CURLY LEAF (CLF) and SWINGER (SWN)<sup>22</sup>. Both CLF and SWN are expressed during postembryonic development and are likely to have redundant functions<sup>23</sup>, whereas MEA expression is limited to the female gametophyte and embryo development<sup>24</sup>. Although CLF and SWN are the only known H3K27 methyltransferases to be expressed in adult plants, H3K27me1 at chromocenters is unaffected in *clf swn* double mutants<sup>18</sup>. Furthermore, a mutation in *FERTILIZATION-INDEPENDENT ENDOSPERM*, the sole *Arabidopsis* homolog of Extra sex combs, also has no effect on H3K27me1 (ref. 18). These results strongly suggest that H3K27 methylation at chromocenters is catalyzed by unknown proteins that are not homologous to E(Z).

Here we show that the *Arabidopsis* proteins ARABIDOPSIS TRITHORAX-RELATED PROTEIN 5 (ATXR5) and ATXR6 act as H3K27 monomethyltransferases *in vitro* and *in vivo*. *atxr5 atxr6* double

<sup>1</sup>Department of Biology, Indiana University, Bloomington, Indiana, USA. <sup>2</sup>Howard Hughes Medical Institute, <sup>3</sup>Department of Molecular, Cell and Developmental Biology, <sup>4</sup>Molecular Biology Institute and <sup>5</sup>Life Sciences Core Curriculum, University of California, Los Angeles, California, USA. Correspondence should be addressed to S.D.M. (michaels@indiana.edu).

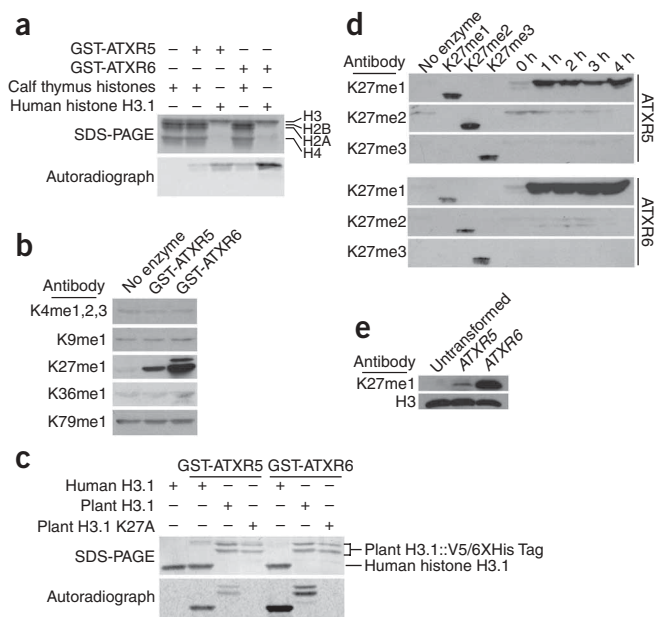


**Figure 1** ATXR5 and ATXR6 monomethylate H3K27. **(a)** *In vitro* HMT assay using radiolabeled SAM. Only H3 is methylated by ATXR5 and ATXR6. **(b)** Products of nonradioactive HMT assays were analyzed by western blotting using antibodies to various methylated lysines of H3. **(c)** *In vitro* HMT assay showing that ATXR5 and ATXR6 cannot methylate a mutant plant H3 protein in which Lys27 is replaced with alanine (K27A). **(d)** ATXR5 and ATXR6 HMT time-course assay products were analyzed by western blotting using antibodies to mono-, di- and trimethylated forms of H3K27. Methylated H3K27 peptides were included to confirm the specificity of the antibodies; a no-enzyme negative control was also included. **(e)** Western blot analysis of histones extracted from *S. cerevisiae* expressing ATXR5 and ATXR6.

lysines of H3. Of these, only the antibody to H3K27me1 detected a strong difference between control and enzyme-treated samples (**Fig. 1b** and **Supplementary Fig. 2**). To confirm that K27 is indeed the residue methylated by ATXR5 and ATXR6, we created a plant H3 variant in which Lys27 is changed to alanine (H3K27A) and repeated the HMT assay. ATXR5 and ATXR6 efficiently methylated the wild-type plant H3 protein, but not H3K27A (**Fig. 1c**).

We then investigated the possibility that ATXR5 and ATXR6 add more than one methyl group to H3K27. The level of H3K27 methylation (mono-, di- or trimethylated) has important functional implications. For example, immunofluorescence experiments in *Arabidopsis* have shown that H3K27me1 is enriched in constitutive heterochromatin, whereas H3K27me3 is restricted to euchromatin<sup>18,19</sup>. We therefore repeated the HMT assay with antibodies that recognize H3K27me1, H3K27me2 and H3K27me3. Even after prolonged incubation, only monomethylation at H3K27 was detected for both ATXR5 and ATXR6 (**Fig. 1d**), suggesting that these proteins function only as H3K27 monomethyltransferases. To obtain additional evidence that ATXR5 and ATXR6 monomethylate H3K27, we expressed ATXR5 and ATXR6 in the budding yeast *Saccharomyces cerevisiae*. This model system is particularly suitable for this experiment, as methylation of H3K27 is either absent or very minimal<sup>33</sup>. Expression of ATXR5 or ATXR6 in yeast did indeed induce monomethylation at Lys27 (**Fig. 1e**). These results show that ATXR5 and ATXR6 are, to our knowledge, the first examples of eukaryotic H3K27 methyltransferases that are not related to the *Drosophila* E(Z) protein.

### ATXR5 and ATXR6 have redundant functions in development

To investigate the functions of ATXR5 and ATXR6 *in vivo*, we obtained T-DNA insertional mutants (*atxr5*, SALK\_130607; *atxr6*, SAIL\_240\_H01 (ref. 34)). The T-DNA insertion in *atxr5* is located in the coding sequence upstream of the SET domain (**Fig. 2a** and **Supplementary Fig. 1**). For *atxr6*, the closest available T-DNA insertion is located 147 base pairs (bp) upstream of the predicted start codon. Semiquantitative RT-PCR analysis showed that the mutants have lower *atxr5* and *atxr6* mRNA levels than do wild-type Columbia plants (**Fig. 2b**). No alterations in growth or development were observed in the single mutants.

Given the similarities in sequence (**Supplementary Fig. 1**) and biochemical activity (**Fig. 1**) and partially overlapping expression patterns (**Fig. 2c**), we suspected that ATXR5 and ATXR6 have redundant functions. We therefore created an *atxr5 atxr6* double mutant. *atxr5 atxr6* plants were smaller than wild-type plants (**Fig. 2d**), especially when grown under short days. This phenotype seems to result primarily from reduced leaf size, as the rate of leaf initiation in mutants was similar to that of wild-type plants (**Fig. 2e**).

### Chromatin condensation and gene silencing require H3K27me1

Because H3K27me1 is associated with constitutive heterochromatin in *Arabidopsis*<sup>18,19</sup>, we examined the effect of *atxr5* and *atxr6* mutations

mutants show reduced H3K27me1 at chromocenters and partial heterochromatin decondensation. In addition, our results clarify the relationship between different epigenetic marks present in heterochromatin and their roles in gene silencing. Transcriptional activation of repressed elements is observed in *atxr5 atxr6* mutant plants, but DNA methylation and H3K9me2 levels remain unchanged. Thus, DNA methylation and H3K9me2 occur independent of H3K27me1, and gene silencing at constitutive heterochromatin requires the presence of both H3K27me1 and DNA methylation–H3K9me2.

## RESULTS

### ATXR5 and ATXR6 function as H3K27 monomethyltransferases

Histone lysine methylation is primarily catalyzed by SET-domain proteins<sup>25</sup>. The substrate specificity of most SET-domain proteins can be predicted by comparing their sequences to those of biochemically characterized proteins. Phylogenetic analysis of 32 SET-domain proteins from *Arabidopsis*, however, showed that the homologous proteins ATXR5 and ATXR6 (**Supplementary Fig. 1**) belong to a divergent, functionally uncharacterized group<sup>22,26</sup>. It is therefore not possible to predict which histone lysine residue is methylated by these two proteins. ATXR5 and ATXR6 seem to be plant specific, and their origin is likely to coincide with the emergence of land plants, as homologs of these proteins are present in the moss *Physcomitrella patens* (**Supplementary Fig. 1**) but not in the unicellular green algae *Chlamydomonas reinhardtii*.

To determine whether ATXR5 and ATXR6 are involved in histone methylation, we conducted *in vitro* histone methyltransferase (HMT) assays. We mixed purified glutathione S-transferase (GST)-tagged ATXR5 and ATXR6 and radiolabeled S-adenosyl methionine (SAM) with calf thymus histones or recombinant human histone H3.1. Both ATXR5 and ATXR6 methylated H3, but not other histone proteins (**Fig. 1a**).

H3 contains four lysine residues that have been reported to be methylated in *Arabidopsis*: Lys4, Lys9, Lys27 and Lys36 (refs. 27,28). In addition, Lys79 is methylated by the non-SET-domain protein Dot1 in yeasts and animals<sup>29–32</sup>. To identify which site is methylated by ATXR5 and ATXR6, we repeated the HMT assay with nonradiolabeled SAM and used antibodies that recognize the five different monomethylated

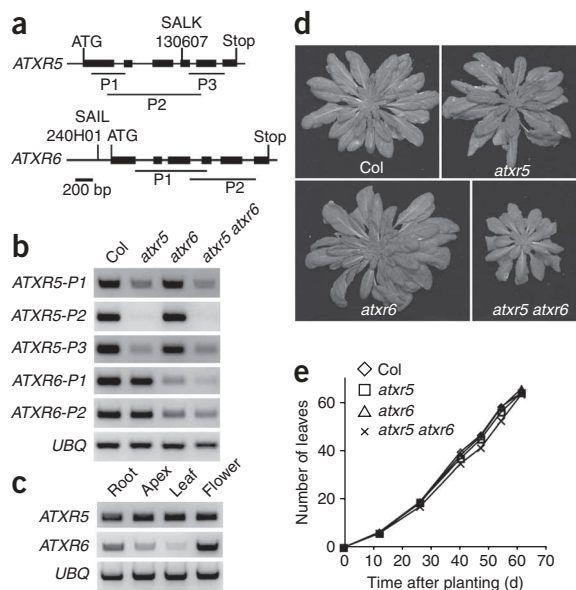


**Figure 2** ATXR5 and ATXR6 have redundant roles in leaf development. (a) Genomic structure of *ATXR5* and *ATXR6*. Thin horizontal lines represent the chromosome, thick lines represent exons, and horizontal lines below represent regions amplified by each primer pair (P1, P2 and P3). (b,c) Semiquantitative RT-PCR analysis of *ATXR5* and *ATXR6* expression in fully expanded leaves (b) and various tissues (c). *UBIQUITIN (UBQ)* was used as a constitutively expressed control. (d) Wild-type (Col) plants and single and double mutants of *atxr5* and *atxr6* grown under short-day conditions. (e) Rates of leaf initiation of plants grown under short days.

release of silencing at a DNA repeat (*TRANSCRIPTIONALLY SILENT INFORMATION*) and transposons (*Ta3*, *AtMu1* and *CACTA*) localized in chromocenters (Fig. 3c). To determine whether the loss of silencing is associated with reduced H3K27me1, we conducted chromatin immunoprecipitation (ChIP) analysis on *TRANSCRIPTIONALLY SILENT INFORMATION*, *Ta3* and *CACTA*. H3K27me1 was reduced at these loci (Fig. 3d), suggesting that ATXR5 and ATXR6 act directly at these elements. Taken together, these results suggest that ATXR5 and ATXR6 have functionally redundant roles in the formation of constitutive heterochromatin and the silencing of heterochromatic elements in *Arabidopsis*.

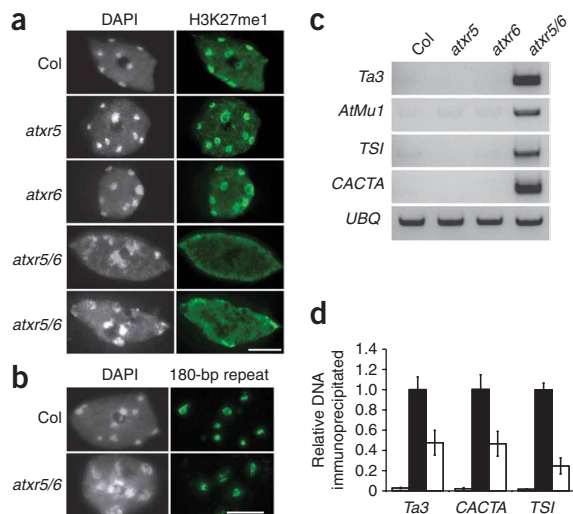
### ATXR5 and ATXR6 are required for heterochromatic H3K27me1

Previous experiments have shown that the enrichment of H3K27me1 at chromocenters does not result from the activities of the known E(Z) homologs MEA, CLF and SWN<sup>18</sup>. To determine whether ATXR5 and/or ATXR6 have a role in H3K27 methylation, we conducted immunocytochemical assays using antibodies specific for the three different methylated forms of H3K27. The specificity of each antibody was confirmed by western blot analysis using methylated H3 peptides (Fig. 1d). Di- and trimethylation were not affected in single or double mutants (Fig. 4a,b). Although previous studies have suggested that H3K27me2 is enriched in chromocenters<sup>18,19</sup>, we did not observe chromocenter staining with the H3K27me2-specific antibody used in this study (Fig. 4a). However, the antibody to H3K27me2 used in previous studies showed substantial cross-reactivity with H3K27me1 (ref. 38). This, together with the observation that H3K27me1 is roughly four times more abundant than H3K27me2 in *Arabidopsis*<sup>27</sup>, led us to suspect that the reported H3K27me2 localization in chromocenters is a result of antibody cross-reaction with H3K27me1. Consistent with this hypothesis, immunostaining with the previously used antibody to H3K27me2 (ref. 38) in the presence

on chromatin structure (Fig. 3). We observed several 4',6-diamidino-2-phenylindole (DAPI)-stained chromocenters, characteristic of constitutive heterochromatin, in nuclei isolated from fully expanded *Arabidopsis* leaves (Fig. 3a,b; see also Figs. 4 and 5). *atxr5* and *atxr6* single mutants showed no visible defects in heterochromatin organization. In contrast, ~65% of *atxr5 atxr6* double-mutant nuclei showed partial decondensation of the chromocenters (Fig. 3a,b; see also Figs. 4 and 5). Mutations in a number of chromatin-modifying and chromatin-associated proteins lead to heterochromatin decondensation<sup>35</sup>. These mutations, however, can have different effects on chromatin structure. For example, *met1* and *decrease in DNA methylation1 (ddm1)* mutants show decondensation of pericentromeric sequences but not of the 180-bp centromeric repeats<sup>35</sup>. In contrast, *variant in methylation1* mutants show decondensation of centromeric sequences<sup>36</sup>. We analyzed the 180-bp repeat sequences by fluorescence *in situ* hybridization (FISH) and found that the centromeric sequences were not strongly decondensed in *atxr5 atxr6* double mutants (Fig. 3b). Thus, the disruptions in heterochromatin structure observed in *atxr5 atxr6* plants seem to be more similar to those observed in *met1* and *ddm1* mutants.

Mutations that affect chromatin structure often lead to transcriptional reactivation of repressed heterochromatic elements<sup>37</sup>. In *atxr5 atxr6* plants, chromatin decondensation was also accompanied by the

**Figure 3** *atxr5 atxr6 (atxr5/6)* mutations lead to disruption of constitutive heterochromatin, reduced H3K27 monomethylation and reactivation of silenced elements. (a) Leaf interphase nuclei were stained with DAPI and analyzed for immunofluorescence with antibody to H3K27me1. Approximately 65% of *atxr5 atxr6* nuclei show severe (upper panel) or moderate (lower panel) chromocenter decondensation and reduced H3K27me1 staining. Scale bar, 5  $\mu$ m. (b) FISH analysis of leaf interphase nuclei using a 180-bp centromeric repeat probe. DNA was counterstained with DAPI. Scale bar, 5  $\mu$ m. (c) Semiquantitative RT-PCR analysis of heterochromatic elements in Columbia, *atxr5*, *atxr6* and *atxr5 atxr6* plants. *UBQ* was used as a constitutively expressed control. (d) ChIP analysis of repetitive elements using antibody to H3K27me1. Black and white bars indicate relative levels of immunoprecipitated DNA normalized to *ACTIN*, as determined by real-time PCR, from wild-type and *atxr5 atxr6* leaves, respectively. Grey bars represent no-antibody controls. Data are presented as mean  $\pm$  s.e.m. for three individual experiments.





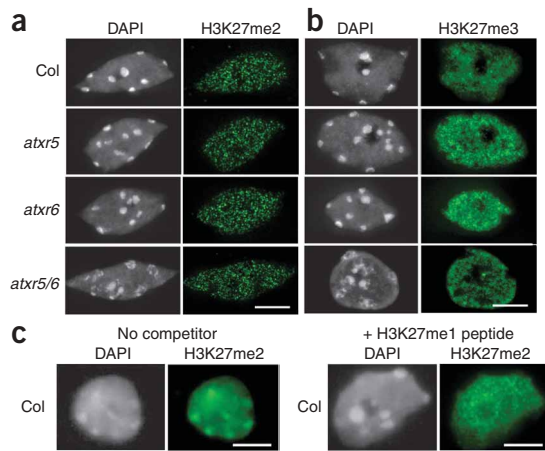


**Figure 4** Di- and trimethylation of H3K27 are not altered in *atxr5 atxr6* mutants. (a,b) Leaf interphase nuclei were stained with DAPI and analyzed for immunofluorescence with antibodies to H3K27me2 (a) and H3K27me3 (b). (c) Leaf interphase nuclei were stained with DAPI and analyzed for immunofluorescence with antibody to H3K27me2 (ref. 38) in the presence or absence of an H3K27me1 peptide. Scale bars, 5  $\mu$ m.

of an H3K27me1 peptide competitor eliminated chromocenter staining (Fig. 4c). These results suggest that the previously reported chromocenter enrichment of H3K27me2 resulted from antibody cross-reactivity with H3K27me1.

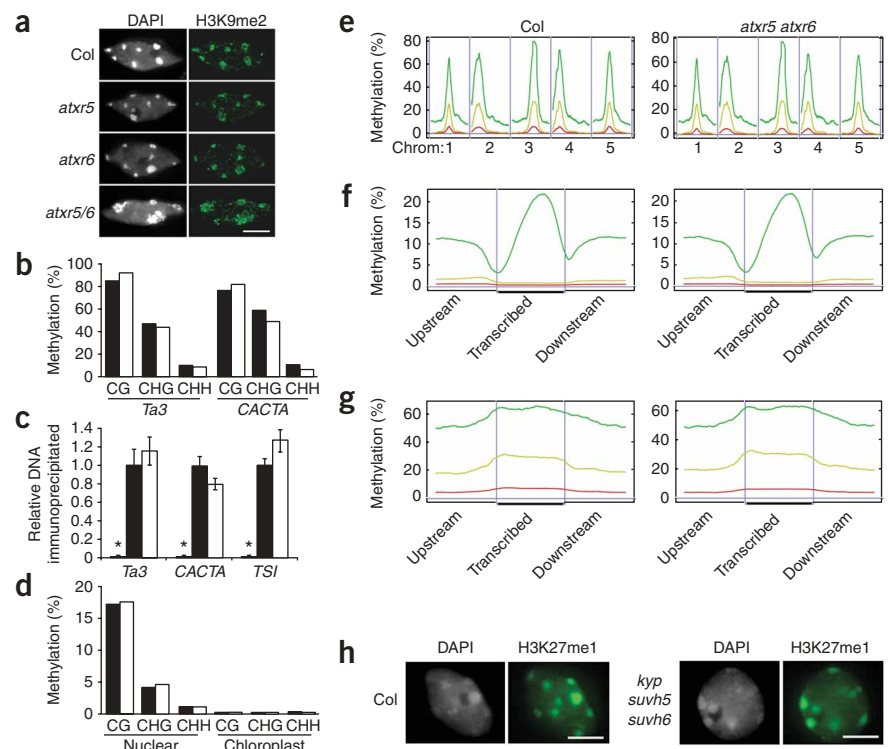
In contrast to di- and trimethylation, H3K27 monomethylation was affected in *atxr5 atxr6* mutants. In wild-type (Columbia) plants, we observed fluorescence throughout the nucleus, with the strongest staining occurring at chromocenters (Fig. 3a). This pattern was unchanged in *atxr5* or *atxr6* single mutants. In the *atxr5 atxr6* double mutant, however, staining was strongly reduced in chromocenters (Fig. 3a), and total H3K27me1 levels were on average 22% lower than wild-type levels (Supplementary Fig. 3). However, H3K27me1 was not always completely eliminated from the chromocenters of *atxr5*

*atxr6* nuclei (Fig. 3a). This may be explained by residual ATXR6 activity, as our mutant allele is not likely to be a null allele (Fig. 2b), or by catalysis of the remaining H3K27me1 by other H3K27 methyltransferases (such as MEA, CLF and SWN). Because H3K27me2 and H3K27me3 were unaffected in *atxr5 atxr6* mutants (Fig. 4a,b), and ChIP coupled with shotgun sequencing did not detect H3K27me3 at *Ta3*, *AtMu1* or *CACTA* (data not shown), we believe the loss of gene silencing and chromatin decondensation in *atxr5 atxr6* mutants results from reduced H3K27me1.

### H3K27me1 does not affect DNA methylation or H3K9me2

In addition to H3K27me1, H3K9me2 and DNA methylation at symmetric (CG and CHG) and asymmetric (CHH) sites are enriched in constitutive heterochromatin and are tightly associated with transcriptional silencing in *Arabidopsis*<sup>17</sup>. The relationships between epigenetic marks are complex. For example, it is well documented that mutations in the enzymes responsible for DNA methylation can affect H3K9 dimethylation, and vice versa<sup>17,37</sup>. Given the observed reactivation of heterochromatic elements, we predicted that the reduction in H3K27me1 in *atxr5 atxr6* double mutants might also be accompanied by reductions in DNA methylation and H3K9me2. Notably, the global distribution of H3K9me2 did not seem to be altered in *atxr5 atxr6* double mutants (Fig. 5a). Also, we did not

**Figure 5** Mutations in *atxr5* and *atxr6* do not affect H3K9 dimethylation or DNA methylation. (a) Leaf interphase nuclei were stained with DAPI and analyzed for immunofluorescence with antibody to H3K9me2. Scale bar, 5  $\mu$ m. (b) DNA methylation analysis by locus-specific (*Ta3* and *CACTA*) BS-Seq. Black and white bars represent wild-type and *atxr5 atxr6* plants, respectively. (c) ChIP analysis of repetitive elements using antibody to H3K9me2. Black and white bars indicate relative levels of immunoprecipitated DNA normalized to *ACTIN*, as determined by real-time PCR, from wild-type and *atxr5 atxr6* plants, respectively. Grey bars represent no-antibody controls. Data are presented as mean  $\pm$  s.e.m. for three individual experiments. (d) DNA methylation analysis by genome-wide BS-Seq. (e) Distribution of methylation along the five *Arabidopsis* chromosomes. (f) Average methylation levels within protein-coding genes. (g) Average methylation levels within pseudogenes and transposons. Horizontal blue lines in e–g indicate 0% methylation, green lines indicate CG methylation, yellow lines indicate CHG methylation and red lines indicate CHH methylation. Vertical blue lines in e separate different chromosomes. Vertical blue lines in f and g mark boundaries between upstream regions and gene bodies and between gene bodies and downstream regions. (h) Leaf interphase nuclei of wild-type and *kyp suvh5 suvh6* triple-mutant plants were stained with DAPI and analyzed for immunofluorescence with antibody to H3K27me1. Scale bars, 5  $\mu$ m.



observe changes in DNA methylation (Fig. 5b) or H3K9me2 (Fig. 5c) at loci that showed reactivation in the *atxr5 atxr6* double mutant, suggesting that the release of silencing in *atxr5 atxr6* double mutants is independent of H3K9me2 and DNA methylation. Because this result was unexpected, we used bisulfite conversion coupled with Illumina/Solexa shotgun sequencing (BS-Seq)<sup>3</sup> to examine DNA methylation at a global level. Consistent with our locus-specific analysis (Fig. 5b), DNA methylation patterns were indeed similar between wild-type plants and *atxr5 atxr6* double mutants across the genome (Fig. 5d–g).

These results indicate that the reduced heterochromatic H3K27me1 in *atxr5 atxr6* double mutants does not affect DNA methylation or H3K9me2. The independence between H3K27me1 and the other epigenetic modifications found at chromocenters seems to be bidirectional, as H3K27me1 levels are not changed in *met1* or *kyp* mutants<sup>18,19</sup>. Recent work has shown that KYP is partially redundant with SUVH5 and SUVH6 in catalyzing the dimethylation of H3K9 (ref. 14). To provide additional evidence that H3K27me1 levels are independent of H3K9me2 levels, we assessed the distribution of H3K27me1 in a *kyp suvh5 suvh6* triple mutant. H3K27me1 at chromocenters was not affected in the triple mutant (Fig. 5h). Thus, H3K27me1 occurs independent of DNA methylation and H3K9me2, and both sets of modifications are required for gene silencing.

## DISCUSSION

In this study, we showed that the divergent SET-domain proteins ATXR5 and ATXR6 are H3K27 methyltransferases that are not homologous to the *Drosophila* protein E(Z). ATXR5 and ATXR6 are the only enzymes that have been shown biochemically to catalyze the methylation of H3K27 in *Arabidopsis*. Despite the fact that MEA, SWN and CLF are also thought to methylate H3K27, given their similarity to E(Z), and the lower H3K27me2 and H3K27me3 levels in mutants<sup>18,22,26,39–41</sup>, these proteins remain biochemically uncharacterized.

The post-translational processing of H3K27 is complex, both in terms of the types of modifications and the spatial distribution of modified forms. H3K27 in *Arabidopsis* exists in H3K27me1, H3K27me2, H3K27me3 and unmethylated (H3K27me0) forms<sup>27,28</sup>. In contrast to some eukaryotes, H3K27 is not acetylated in *Arabidopsis*<sup>28</sup>. Although all methylated forms of H3K27 are associated with transcriptional repression (this study and ref. 42), immunostaining reveals distinct nuclear localization patterns; H3K27me1 is enriched in constitutive heterochromatin, whereas H3K27me2 and H3K27me3 are primarily localized to euchromatin (this study and refs. 18,19). Thus, three remaining unknowns regarding H3K27 methylation are the mechanisms by which the various methylation states are generated, the way in which they are localized to particular regions of the genome, and the functional differences between the different methylated forms.

The data presented here indicate that ATXR5 and ATXR6 are only involved in H3K27 monomethylation. H3K27me1 is reduced at heterochromatin in *atxr5 atxr6* double mutants. Consistent with this result, ATXR5 and ATXR6 show only H3K27 monomethyltransferase activity *in vitro*. This strongly suggests that the primary role of ATXR5 and ATXR6 is in H3K27 monomethylation and that other enzymes are responsible for H3K27me2 and H3K27me3. Di- and trimethylation of H3K27 is likely to be carried out by MEA, SWN and CLF. Although the enzymatic activity of MEA, SWN and CLF has not been established biochemically, these proteins are present in PRC2-like complexes in *Arabidopsis*<sup>43,44</sup>. The PRC2 complex is highly conserved and

is responsible for H3K27me2 and H3K27me3 in many eukaryotes<sup>20,45,46</sup>. Our results indicate that monomethylation of H3K27 by ATXR5 and ATXR6 is not required before di- and trimethylation of H3K27, as H3K27me2 and H3K27me3 levels are not affected in *atxr5 atxr6* mutants. This suggests that MEA, SWN and CLF are able to catalyze the formation of H3K27me2 and H3K27me3 directly from H3K27me0.

Although ATXR5 and ATXR6 contribute to H3K27me1 levels in chromocenters, we observed that this histone mark is only ~22% lower overall in *atxr5 atxr6* double mutants. The remaining H3K27me1 could result from residual ATXR6 activity, as the allele used in this study is not a null allele. Another explanation that is not mutually exclusive is that some H3K27me1 may be catalyzed by MEA, SWN and CLF, either directly through monomethyltransferase activity or indirectly through the conversion of H3K27me2 and H3K27me3 to H3K27me1 by histone demethylases. Although the chromocenter enrichment of H3K27me1 is clearly visible by immunostaining, it remains unclear whether this mark is also abundant in euchromatin. In mammals, H3K27me1 is enriched, as in *Arabidopsis*, at the pericentromeric heterochromatin<sup>38</sup>. It is also broadly distributed in euchromatin, with the exception of regions surrounding the transcription start site of active genes<sup>47</sup>. Some evidence suggests that H3K27me1 is also found outside of the constitutive heterochromatin in plants. In the gymnosperms *Pinus sylvestris* and *Picea abies*, H3K27me1 is uniformly distributed along the complete length of all chromosomes<sup>48</sup>. In *Arabidopsis*, it is possible that the heterochromatic enrichment of H3K27me1, as observed by immunostaining, results in part from the compact structure of the chromocenters. Precise mapping of H3K27me1 in the *Arabidopsis* genome will be needed to determine the prevalence of this mark outside of the constitutive heterochromatin.

In addition to their SET domains, ATXR5 and ATXR6 each contain a plant homeodomain (PHD) domain and a PROLIFERATING CELL NUCLEAR ANTIGEN (PCNA)-interacting protein box<sup>49</sup>. Given the role of ATXR5 and ATXR6 in catalyzing H3K27me1 at the chromocenters, the mechanism by which their activity is targeted to heterochromatin remains to be determined. Some PHD domains mediate interactions with specific post-translationally modified forms of H3 (refs. 50,51). The PHD domains of ATXR5 and ATXR6 could direct the activity of these proteins to chromocenters by interacting with specific forms of H3 that are enriched in heterochromatin. Further studies on ATXR5 and ATXR6 may also shed light on how the H3K27me1 mark is maintained through DNA replication. Given that ATXR5 and ATXR6 are likely to interact directly with PCNA during the S phase of the cell cycle<sup>49</sup>, it is possible that these proteins modify newly synthesized histones that are incorporated into heterochromatin during DNA synthesis. This model could help to explain the epigenetic inheritance of H3K27me1 in *Arabidopsis*. SETDB1 and G9A are two examples of HMTs that localize at the replication fork in mammals<sup>52,53</sup>.

In conclusion, ATXR5 and ATXR6 comprise a class of H3K27 methyltransferases with crucial roles in H3K27 monomethylation, chromatin condensation and gene silencing in *Arabidopsis*. Our results, in combination with previous studies showing that H3K27me1 levels are unchanged in mutants with altered DNA methylation or H3K9 methyltransferase activity<sup>18,19</sup>, indicate that H3K27me1 and DNA methylation–H3K9me2 are two essential and independent pathways required for the silencing of heterochromatic elements in *Arabidopsis*. These two pathways are also required to regulate the structural organization of chromocenters. Future work is required to understand

the extent to which the two pathways overlap and the biological mechanisms for which they provide unique functions.

## METHODS

Methods and any associated references are available in the online version of the paper at <http://www.nature.com/nsmb/>.

**Accession codes.** Gene Expression Omnibus: BS-seq data sets have been deposited under accession number GSE16071.

*Note: Supplementary information is available on the Nature Structural & Molecular Biology website.*

## ACKNOWLEDGMENTS

We thank C.E. Walczak for assistance with microscopy. This work was supported by grants to S.D.M. from the National Science Foundation (IOB-0447583) and National Institutes of Health (GM075060); to Y.J. from the Fonds québécois de recherche sur la nature et les technologies; and to Y.V.B. from the US Public Health Service (National Research Service award GM07104). Research in the laboratory of S.E.J. was supported by National Institutes of Health grant GM60398. S.E.J. is an investigator of the Howard Hughes Medical Institute.

## AUTHOR CONTRIBUTIONS

Y.J. carried out the genetic and biochemical characterization of ATXR5 and ATXR6. Y.J. and C.A.L. generated the gene expression and ChIP data. S.F. generated and sequenced the BS-Seq libraries. Y.V.B. conducted the locus-specific bisulfite sequencing analyses. H.S. validated the ChIP and RT-PCR results. C.A.L., Y.V.B. and L.M.J. conducted the immunofluorescence studies. S.C., M.P., S.F. and S.E.J. analyzed the BS-Seq data. S.D.M., M.P. and S.E.J. participated in the design of experiments.

Published online at <http://www.nature.com/nsmb/>

Reprints and permissions information is available online at <http://npg.nature.com/reprintsandpermissions/>

- Li, B., Carey, M. & Workman, J.L. The role of chromatin during transcription. *Cell* **128**, 707–719 (2007).
- Maluszynska, J. & Heslop-Harrison, J.S. Localization of tandemly repeated DNA sequences in *Arabidopsis thaliana*. *Plant J.* **1**, 159–166 (1991).
- Cokus, S.J. *et al.* Shotgun bisulphite sequencing of the *Arabidopsis* genome reveals DNA methylation patterning. *Nature* **452**, 215–219 (2008).
- Johnson, L., Cao, X. & Jacobsen, S. Interplay between two epigenetic marks. DNA methylation and histone H3 lysine 9 methylation. *Curr. Biol.* **12**, 1360–1367 (2002).
- Probst, A.V., Fransz, P.F., Paszkowski, J. & Mittelsten Scheid, O. Two means of transcriptional reactivation within heterochromatin. *Plant J.* **33**, 743–749 (2003).
- Tariq, M. *et al.* Erasure of CpG methylation in *Arabidopsis* alters patterns of histone H3 methylation in heterochromatin. *Proc. Natl. Acad. Sci. USA* **100**, 8823–8827 (2003).
- Zhang, X. *et al.* Whole-genome analysis of histone H3 lysine 27 trimethylation in *Arabidopsis*. *PLoS Biol.* **5**, e129 (2007).
- Cao, X. & Jacobsen, S.E. Locus-specific control of asymmetric and CpNpG methylation by the DRM and CMT3 methyltransferase genes. *Proc. Natl. Acad. Sci. USA* **99**, S16491–S16498 (2002).
- Cao, X. & Jacobsen, S.E. Role of the *Arabidopsis* DRM methyltransferases in *de novo* DNA methylation and gene silencing. *Curr. Biol.* **12**, 1138–1144 (2002).
- Ronemus, M.J., Galbiati, M., Ticknor, C., Chen, J. & Dellaporta, S.L. Demethylation-induced developmental pleiotropy in *Arabidopsis*. *Science* **273**, 654–657 (1996).
- Jackson, J.P., Lindroth, A.M., Cao, X. & Jacobsen, S.E. Control of CpNpG DNA methylation by the KRYPTONITE histone H3 methyltransferase. *Nature* **416**, 556–560 (2002).
- Finnegan, E.J. & Dennis, E.S. Isolation and identification by sequence homology of a putative cytosine methyltransferase from *Arabidopsis thaliana*. *Nucleic Acids Res.* **21**, 2383–2388 (1993).
- Ebbs, M.L., Bartee, L. & Bender, J. H3 lysine 9 methylation is maintained on a transcribed inverted repeat by combined action of SUVH6 and SUVH4 methyltransferases. *Mol. Cell. Biol.* **25**, 10507–10515 (2005).
- Ebbs, M.L. & Bender, J. Locus-specific control of DNA methylation by the *Arabidopsis* SUVH5 histone methyltransferase. *Plant Cell* **18**, 1166–1176 (2006).
- Naumann, K. *et al.* Pivotal role of AtSUVH2 in heterochromatic histone methylation and gene silencing in *Arabidopsis*. *EMBO J.* **24**, 1418–1429 (2005).
- Malagnac, F., Bartee, L. & Bender, J. An *Arabidopsis* SET domain protein required for maintenance but not establishment of DNA methylation. *EMBO J.* **21**, 6842–6852 (2002).
- Vaillant, I. & Paszkowski, J. Role of histone and DNA methylation in gene regulation. *Curr. Opin. Plant Biol.* **10**, 528–533 (2007).
- Lindroth, A.M. *et al.* Dual histone H3 methylation marks at lysines 9 and 27 required for interaction with CHROMOMETHYLASE3. *EMBO J.* **23**, 4146–4155 (2004).
- Mathieu, O., Probst, A.V. & Paszkowski, J. Distinct regulation of histone H3 methylation at lysines 27 and 9 by CpG methylation in *Arabidopsis*. *EMBO J.* **24**, 2783–2791 (2005).
- Müller, J. *et al.* Histone methyltransferase activity of a *Drosophila* Polycomb group repressor complex. *Cell* **111**, 197–208 (2002).
- Ketel, C.S. *et al.* Subunit contributions to histone methyltransferase activities of fly and worm Polycomb group complexes. *Mol. Cell. Biol.* **25**, 6857–6868 (2005).
- Baumbusch, L.O. *et al.* The *Arabidopsis thaliana* genome contains at least 29 active genes encoding SET domain proteins that can be assigned to four evolutionarily conserved classes. *Nucleic Acids Res.* **29**, 4319–4333 (2001).
- Chanvittana, Y. *et al.* Interaction of Polycomb-group proteins controlling flowering in *Arabidopsis*. *Development* **131**, 5263–5276 (2004).
- Grossniklaus, U., Vielle-Calzada, J.P., Hoepfner, M.A. & Gagliano, W.B. Maternal control of embryogenesis by MEDEA, a Polycomb group gene in *Arabidopsis*. *Science* **280**, 446–450 (1998).
- Rea, S. *et al.* Regulation of chromatin structure by site-specific histone H3 methyltransferases. *Nature* **406**, 593–599 (2000).
- Springer, N.M. *et al.* Comparative analysis of SET domain proteins in maize and *Arabidopsis* reveals multiple duplications preceding the divergence of monocots and dicots. *Plant Physiol.* **132**, 907–925 (2003).
- Johnson, L. *et al.* Mass spectrometry analysis of *Arabidopsis* histone H3 reveals distinct combinations of post-translational modifications. *Nucleic Acids Res.* **32**, 6511–6518 (2004).
- Zhang, K., Sridhar, V.V., Zhu, J., Kapoor, A. & Zhu, J.K. Distinctive core histone post-translational modification patterns in *Arabidopsis thaliana*. *PLoS One* **2**, e1210 (2007).
- van Leeuwen, F., Gafken, P.R. & Gottschling, D.E. Dot1p modulates silencing in yeast by methylation of the nucleosome core. *Cell* **109**, 745–756 (2002).
- Ng, H.H. *et al.* Lysine methylation within the globular domain of histone H3 by Dot1 is important for telomeric silencing and Sir protein association. *Genes Dev.* **16**, 1518–1527 (2002).
- Lacoste, N., Utley, R.T., Hunter, J.M., Poirier, G.G. & Cote, J. Disruptor of telomeric silencing-1 is a chromatin-specific histone H3 methyltransferase. *J. Biol. Chem.* **277**, 30421–30424 (2002).
- Feng, Q. *et al.* Methylation of H3-lysine 79 is mediated by a new family of HMTases without a SET domain. *Curr. Biol.* **12**, 1052–1058 (2002).
- Garcia, B.A. *et al.* Organismal differences in post-translational modifications in histones H3 and H4. *J. Biol. Chem.* **282**, 7641–7655 (2007).
- Alonso, J.M. *et al.* Genome-wide insertional mutagenesis of *Arabidopsis thaliana*. *Science* **301**, 653–657 (2003).
- Soppe, W.J. *et al.* DNA methylation controls histone H3 lysine 9 methylation and heterochromatin assembly in *Arabidopsis*. *EMBO J.* **21**, 6549–6559 (2002).
- Woo, H.R., Pontes, O., Pikaard, C.S. & Richards, E.J. VIM1, a methylcytosine-binding protein required for centromeric heterochromatinization. *Genes Dev.* **21**, 267–277 (2007).
- Henderson, I.R. & Jacobsen, S.E. Epigenetic inheritance in plants. *Nature* **447**, 418–424 (2007).
- Peters, A.H. *et al.* Partitioning and plasticity of repressive histone methylation states in mammalian chromatin. *Mol. Cell* **12**, 1577–1589 (2003).
- Makarevich, G. *et al.* Different Polycomb group complexes regulate common target genes in *Arabidopsis*. *EMBO Rep.* **7**, 947–952 (2006).
- Schönrock, N. *et al.* Polycomb-group proteins repress the floral activator AGL19 in the FLC-independent vernalization pathway. *Genes Dev.* **20**, 1667–1678 (2006).
- Schubert, D. *et al.* Silencing by plant Polycomb-group genes requires dispersed trimethylation of histone H3 at lysine 27. *EMBO J.* **25**, 4638–4649 (2006).
- Köhler, C. & Grossniklaus, U. Epigenetic inheritance of expression states in plant development: the role of Polycomb group proteins. *Curr. Opin. Cell Biol.* **14**, 773–779 (2002).
- De Lucia, F., Crevillen, P., Jones, A.M., Greb, T. & Dean, C. A PHD-polycomb repressive complex 2 triggers the epigenetic silencing of FLC during vernalization. *Proc. Natl. Acad. Sci. USA* **105**, 16831–16836 (2008).
- Wood, C.C. *et al.* The *Arabidopsis thaliana* vernalization response requires a Polycomb-like protein complex that also includes VERNALIZATION INSENSITIVE 3. *Proc. Natl. Acad. Sci. USA* **103**, 14631–14636 (2006).
- Reyes, J.C. & Grossniklaus, U. Diverse functions of Polycomb group proteins during plant development. *Semin. Cell Dev. Biol.* **14**, 77–84 (2003).
- Lee, T.I. *et al.* Control of developmental regulators by Polycomb in human embryonic stem cells. *Cell* **125**, 301–313 (2006).
- Vakoc, C.R., Sachdeva, M.M., Wang, H. & Blobel, G.A. Profile of histone lysine methylation across transcribed mammalian chromatin. *Mol. Cell. Biol.* **26**, 9185–9195 (2006).
- Fuchs, J., Jovtchev, G. & Schubert, I. The chromosomal distribution of histone methylation marks in gymnosperms differs from that of angiosperms. *Chromosome Res.* **16**, 891–898 (2008).
- Raynaud, C. *et al.* Two cell-cycle regulated SET-domain proteins interact with proliferating cell nuclear antigen (PCNA) in *Arabidopsis*. *Plant J.* **47**, 395–407 (2006).
- Shi, X. *et al.* ING2 PHD domain links histone H3 lysine 4 methylation to active gene repression. *Nature* **442**, 96–99 (2006).
- Wysocka, J. *et al.* A PHD finger of NURF couples histone H3 lysine 4 trimethylation with chromatin remodelling. *Nature* **442**, 86–90 (2006).
- Estève, P.O. *et al.* Direct interaction between DNMT1 and G9a coordinates DNA and histone methylation during replication. *Genes Dev.* **20**, 3089–3103 (2006).
- Sarraf, S.A. & Stancheva, I. Methyl-CpG binding protein MBD1 couples histone H3 methylation at lysine 9 by SETDB1 to DNA replication and chromatin assembly. *Mol. Cell* **15**, 595–605 (2004).



## ONLINE METHODS

**Plant material.** *atx5* (SALK\_130607) and *atx6* (SAIL\_240\_H01) on the Columbia genetic background were obtained from the *Arabidopsis* Biological Resource Center. Plants were grown under cool-white fluorescent light ( $\sim 100 \mu\text{mol m}^{-2} \text{s}^{-1}$  under long-day (16 h of light followed by 8 h of darkness) or short-day (8 h of light followed by 16 h of darkness) conditions.

**Gene expression analysis.** For semiquantitative RT-PCR analysis, we carried out reverse transcription and PCR as described<sup>54</sup>, with slight modifications. We used 5  $\mu\text{g}$  of RNA for cDNA synthesis and GoTaq DNA Polymerase (Promega) for amplification. The data shown are representative of at least three independent experiments. The primers and PCR conditions are shown in **Supplementary Table 1**.

**Antibodies.** Antibodies used for the HMT assays, ChIP assays and immunostaining were from Millipore (H3K4me1,2,3, 05-791; H3K9me1, 07-450; H3K27me1, 07-448; H3K27me3, 07-449; H3, 07-690) and Abcam (H3K9me2, ab1220; H3K27me2, ab24684; H3K36me1, ab9048; H3K79me1, ab2886). Antibodies for western blots were used according to the manufacturer's recommendations.

**Chromatin immunoprecipitation.** We conducted ChIP assays as described<sup>4</sup>. For the experiments, we used 300 mg of fully expanded leaves and 4.5  $\mu\text{g}$  of antibodies to H3K27me1 or H3K9me2.

**Locus-specific bisulfite sequencing.** Columbia and *atx5 atx6* DNA (350–550 ng) were treated with bisulfite using an EZ DNA Methylation-Gold kit (Zymo Research) according to the manufacturer's instructions. We used 1  $\mu\text{l}$  of bisulfite-treated DNA for PCR with *Ta3-* and *CACTA-*specific primers (no. 1274, 5'-CCACTRATTCCTRAAACACAACATTTCTRTRATA-3'; no. 1269, 5'-GAGAATYAGGTTAATAAGAAAGTGAAGTGT-3'; no. 6059, 5'-AACATCC TTTCCTTCAACTTAACATCACACTC-3'; no. 6076, 5'-ATAGATGAGTTATTT GTTAGTTTTGGTYGTGTTGGTT-3'). PCR products were gel-purified and cloned into a pCR4 Blunt TOPO vector (Invitrogen). A total of 19–27 clones were sequenced for each genotype and locus.

**Genomic bisulfite sequencing and methylation data analysis.** We generated whole-genome shotgun bisulfite-treated DNA libraries using a published protocol<sup>3</sup>, except that we used a plant DNeasy Maxi kit (Qiagen) to isolate *Arabidopsis* genomic DNA. Ultra-high-throughput sequencing of libraries on an Illumina/Solexa 1G genome analyzer was carried out according to the manufacturer's instructions. Sequencing data were first processed using the initial steps of version 0.2.2.4 of the Solexa analysis pipeline and then by

previously published customized software for base calling, bisulfite alignment and nonconversion filtration<sup>3</sup>. In total, 1,858,393 and 1,534,127 aligned 31-bp reads were obtained for wild-type (Columbia) *Arabidopsis* and *atx5 atx6* double mutants, respectively. Methylated cytosines were identified as cytosines (or guanines, as appropriate) in reads aligned to genomic cytosines, whereas unmethylated cytosines were identified as thymines (or adenines, as appropriate) in reads aligned to genomic cytosines. Chromosomal views and metaplots in **Figure 5e–g** were produced as described in a previous report<sup>3</sup>.

**Constructs.** We used pGEX-6P to clone ATXR5 (residues 57–379, PHD-SET; residues 57–133, PHD only) and ATXR6 (residues 25–349, PHD-SET; residues 25–103, PHD only) for HMT assays. For the plant H3 constructs, *At1g09200* was used as a template to amplify a plant H3.1 gene. The resulting PCR fragment was cloned into pENTR/D (Invitrogen) and subcloned into pET-DEST42 (Invitrogen). The K27A mutation was engineered by overlapping PCR. The primers used for construction of the plasmids are available upon request.

**Histone methyltransferase assay.** For HMT assays, 10  $\mu\text{g}$  of calf thymus histones (Roche), 2.5  $\mu\text{g}$  of recombinant human H3.1 (New England Biolabs) or 2.5  $\mu\text{g}$  of plant H3.1 (wild-type or mutant) were incubated with 5  $\mu\text{g}$  of GST-ATXR5 or GST-ATXR6 in 40  $\mu\text{l}$  of methylation buffer (50 mM Tris-HCl (pH 8.5), 20 mM KCl, 10 mM MgCl<sub>2</sub>, 10 mM  $\beta$ -mercaptoethanol and 250 mM sucrose) supplemented with 250 nCi of [<sup>14</sup>C]SAM (GE Life Sciences) or 5 nmol of unlabeled SAM (Sigma) for 3 h at 30 °C. Reactions were stopped by adding 5 $\times$  SDS-PAGE sample buffer, followed by heating to 95 °C for 5 min. After SDS-PAGE on 12% or 15% gels and transfer to PVDF membranes, detection was done using a PhosphorImager or western blotting with antibodies to H3.

**Detection of histone modifications in yeast.** pYES-DEST52-ATXR5 and pYES-DEST52-ATXR6 were transformed into an INVSc1 yeast strain (Invitrogen) and expressed according to the manufacturer's recommendations. Yeast cells were collected 18 h after induction. Nuclear proteins were extracted from yeast cells as described previously<sup>55</sup> and analyzed by western blotting.

**Protein expression, immunofluorescence and FISH analysis.** These experiments are described in **Supplementary Methods**.

54. Michaels, S.D., Bezerra, I.C. & Amasino, R.M. FRIGIDA-related genes are required for the winter-annual habit in *Arabidopsis*. *Proc. Natl. Acad. Sci. USA* **101**, 3281–3285 (2004).

55. Kizer, K.O., Xiao, T. & Strahl, B.D. Accelerated nuclei preparation and methods for analysis of histone modifications in yeast. *Methods* **40**, 296–302 (2006).